C. R. Mecanique 345 (2017) 239–247

Contents lists available at ScienceDirect

Comptes Rendus Mecanique

www.sciencedirect.com

# A method for the identification of dynamic constraint parameters in multi-supported flexible structures

Ahmad Baklouti [a,b,*], José Antunes [a], Vincent Debut [a], Tahar Fakhkakh [b], Mohamed Haddar [b]

[a] Centro de Ciências e Tecnologias Nucleares, Instituto Superior Técnico, Universidade de Lisboa, Estrada Nacional 10, Km 139.7, 2695-066 Bobadela LRS, Portugal

[b] Laboratory of Mechanics Modeling and Production (LA2MP), National School of Engineers of Sfax, University of Sfax, BP N° 1173-3038, Sfax, Tunisia

ARTICLE INFO

*Article history:*
Received 7 December 2016
Accepted 8 February 2017
Available online 14 March 2017

*Keywords:*
Identification of support parameters
Regularization of inverse problems
Multi-supported structures
Structural modifications

ABSTRACT

In this paper, a new method for identifying the dynamical parameters of local constraining supports such as mass, stiffness, and damping was developed through combining the measured frequency transfer functions and structural modification techniques. Since measurement noise often leads to erroneous identifications, regularization techniques have been implemented to reduce noise amplification in the inverse problem. The developed technique has been validated by numerical tests on a multi-supported flexible structure, which can be seen as an idealized electricity generator rotor shaft. The results are satisfactory for noise-free data as well as under realistic noise levels. The sensitivity of the identified support features to noise levels is asserted through a parametric study



## 1. Introduction

Rotors such as gas turbines, centrifugal compressors and fans are among the most important mechanical components in many engineering fields. High-speed rotating machines are often required; yet, they become prone to vibration issues and dynamic instabilities when reaching critical speed regimes. Thus, for reliability reasons, it is necessary to ensure a good stability of the machinery. Hence, rotor instability causes have been investigated for many decades. Newkirk [1] described the “oil whip” phenomenon for the bearing induced instability. It has been shown later that rotor instability can be related to the bearing dynamic coefficients. Stiffness and damping coefficients of the bearings must be known in order to create the rotor’s design, as shown by Ramsden [2]. Further conclusions were then made by Dawson and Taylor [3] through experiments on rotor dynamics, which are required to study the bearings and supports effects on the rotor response. Thermal and elastic distortion effects must be also taken into account and, to this end, the characterization of the dynamic behavior of the bearings is needed. Nordmann and Scholhom [4] proposed a procedure to identify the stiffness and damping parameters of a plain bearing. For rotors mounted on two symmetrical bearings, the impact method was used by Chan and White [5] to identify the dynamic bearing parameters, by adjusting the resulting model on the frequency response functions (FRFs). As bearing parameters are not symmetrical in most cases, the use of their method is restricted. A method for the identification

* Corresponding author at: Laboratory of Mechanics Modeling and Production (LA2MP), National School of Engineers of Sfax, University of Sfax, BP N° 1173-3038, Sfax, Tunisia.
*E-mail address:* Ahmadbaklouti90@gmail.com (A. Baklouti).

http://dx.doi.org/10.1016/j.crme.2017.02.002
1631-0721/

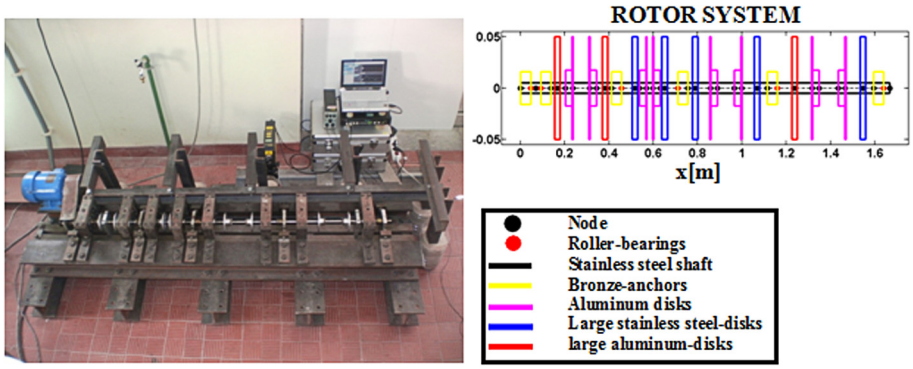


**Fig. 1.** Picture of the rotor test rig at LDA of IST/CTN (left); detailed sketch of the components of the rotor model (right).

of the structural parameters of joints was later proposed by Wang and Liu [6], then extended by Ammugam et al. [7] to identify the linearized parameters of an oil film by using experimental or theoretical FRFs. Qiu and Tieu [8] developed an algorithm to identify the dynamic parameters of a bearing from its impulse response. Chen and Lee [9] proposed a method to estimate the linearized coefficients of rolling element bearings, using the relations of unbalance responses and known system parameters to predict the coefficients of the rolling element bearings. Tiwari et al. [10] proposed an identification algorithm to characterize bearing dynamic properties in a flexible rotor-bearing system, based on unbalance responses. Experimental identification of the dynamic parameters of bearings and seals was further detailed by Tiwari et al. [11]. De Santiago and San Andrés [12] used recorded transient rotor responses, due to impact and unbalance, to identify the bearing support parameters. Tiwari and Chakravarthy [13] presented two identification algorithms to predict the residual unbalance and bearing parameters in a rigid rotor-bearing system. Han et al. [14] suggested an iterative method, based on a Kriging surrogate model and evolutionary algorithm to identify the bearing properties in a rotor-bearing system.

In the present paper, a method for the identification of local structural characteristics, based on the formulation of structural modifications previously proposed by Özgüven [15] and Debut et al. [16] is further developed and applied. It is used for the identification of the linearized support parameters – i.e. mass, stiffness and damping of each rotor bearing – from the computed modal frequencies and mode shapes of the unconstrained rotor and from a measured FRF matrix of the transfer functions relating the dynamics at all support locations of the constrained rotor. The main idea of this method is to exploit a dynamical formulation that relates the unconstrained system to the constrained system. The unconstrained system is represented by means of the transfer functions computed by the finite element method, whereas the constrained one is represented by the measured transfer functions at the supports. The presence of noise in the measurements of transfer functions, as well as almost nodal values in the mode shapes, lead to ill-posed inverse problems. The proposed formulation allows a better regularization of the inverse problem through filtering techniques, namely using singular values decomposition (SVD) of the relevant formulation matrices. Inverse problems of the type addressed here are typically solved through iterative formulations in a nonlinear fashion, and solved using optimization methods. However, these methods become time consuming when the number of the identified parameters increases. Moreover, convergence to a suitable solution is not guaranteed. Therefore, a transformed linear formulation is rather used to find solutions of the inverse problem. Another advantage of the proposed approach is that it does not imply an experimental identification of the constrained modes of the system, which can be delicate in practice. Instead, it is rooted only on transfer function measurements.

As a first step to the problem addressed, this paper presents identification results obtained using realistic simulated data for a model of an electricity generator shaft, under non-rotating conditions. In order to illustrate the satisfactory behavior of the approach, a parametric study is performed to determine the sensitivity of the identification procedure to measurement noise.

## 2. Theoretical model

### 2.1. Description of the proposed approach

The structure is composed of a multiple spans rotor, supported by ball bearings, connected to a fixed structure as shown in Fig. 1. As a first step, we consider that the structure is unconstrained, meaning that boundary conditions at the supports are not taken into account. Then, the frequency transfer function matrix $\mathbf{H}_{\mathbf{U}_{ij}}(\omega)$, which relates the excitation at location $i$ to the response at location $j$, is given in terms of the assembled matrices from the Finite Element model as:

$$\mathbf{H}_{\mathbf{U}}(\omega) = \left[-\omega^2\mathbf{M} + \mathrm{i}\omega\mathbf{C} + \mathbf{K}\right]^{-1} \tag{1}$$

where $\mathbf{M}$, $\mathbf{C}$ and $\mathbf{K}$ are the structure mass, damping and stiffness matrices, respectively. If the supports are considered as localized additional mass, stiffness and damping constraints, then the frequency transfer function matrix $\mathbf{H}_{\mathbf{C}}(\omega)$ of the constrained system can be given by:

$$\begin{aligned}\mathbf{H_C}(\omega) &= \left[-\omega^2\mathbf{M} + \mathrm{i}\omega\mathbf{C} + \mathbf{K} + \left[-\omega^2\mathbf{M_C} + \mathrm{i}\omega\mathbf{C_C} + \mathbf{K_C}\right]\right]^{-1} \\ &= \left[\mathbf{H_U}(\omega)^{-1} + \left[-\omega^2\mathbf{M_C} + \mathrm{i}\omega\mathbf{C_C} + \mathbf{K_C}\right]\right]^{-1}\end{aligned} \tag{2}$$

where matrices $\mathbf{M_C}$, $\mathbf{K_C}$ and $\mathbf{C_C}$ contain the parameters of the supports. As it was shown in a previous work [17], the significantly different orders of magnitude of the support properties (mass, damping, and stiffness) may lead to erroneous identification results. Hence, it is more convenient to use a dimensionless form for the variables. All following equations will be given in terms of dimensionless quantities, as defined below:

$$\tilde{\mathbf{M}}_\mathbf{U} = \frac{1}{m_{U_s}}\mathbf{M_U};\quad \tilde{\mathbf{C}}_\mathbf{U} = \frac{1}{m_{U_s}\omega_{U_s}}\mathbf{C_U};\quad \tilde{\mathbf{K}}_\mathbf{U} = \frac{1}{m_{U_s}\omega_{U_s}^2}\mathbf{K_U} \tag{3}$$

$$\tilde{\mathbf{H}}_\mathbf{U}(\tilde{\omega}) = m_{U_s}\omega_{U_s}^2\mathbf{H_U}(\omega) \tag{4}$$

where $\omega_{U_s}$ and $m_{U_s}$ stand for a reference modal frequency and the corresponding modal mass of the unconstrained system. In terms of dimensionless quantities, the reduced frequency is represented as $\tilde{\omega} = \omega/\omega_{U_s}$. Then, Eq. (1) is reformulated as follows:

$$\tilde{\mathbf{H}}_\mathbf{U}(\tilde{\omega}) = \left[-\tilde{\omega}^2\tilde{\mathbf{M}}_\mathbf{U} + \mathrm{i}\tilde{\omega}\tilde{\mathbf{C}}_\mathbf{U} + \tilde{\mathbf{K}}_\mathbf{U}\right]^{-1} \tag{5}$$

Similarly, from Eq. (2), the frequency transfer function matrix $\mathbf{H_C}(\omega)$ of the constrained system can be written in terms of dimensionless parameters as follows:

$$\tilde{\mathbf{H}}_\mathbf{C}(\tilde{\omega}) = \left[\tilde{\mathbf{H}}_\mathbf{U}(\tilde{\omega})^{-1} + \left[-\tilde{\omega}^2\tilde{\mathbf{M}}_\mathbf{C} + \mathrm{i}\tilde{\omega}\tilde{\mathbf{C}}_\mathbf{C} + \tilde{\mathbf{K}}_\mathbf{C}\right]\right]^{-1} \tag{6}$$

where

$$\tilde{\mathbf{M}}_\mathbf{C} = \frac{1}{m_{U_s}}\mathbf{M_C};\quad \tilde{\mathbf{C}}_\mathbf{C} = \frac{1}{m_{U_s}\omega_{U_s}}\mathbf{C_C};\quad \tilde{\mathbf{K}}_\mathbf{C} = \frac{1}{m_{U_s}\omega_{U_s}^2}\mathbf{K_C} \tag{7}$$

$$\tilde{\mathbf{H}}_\mathbf{C}(\tilde{\omega}) = m_{U_s}\omega_{U_s}^2\mathbf{H_C}(\omega) \tag{8}$$

represent the dimensionless supports parameter matrices and the dimensionless constrained transfer function matrix. From Eq. (2), an estimate of the constrained transfer function matrix $\mathbf{H_C}(\omega)$ may be obtained from the unconstrained dynamics $\mathbf{H_U}(\omega)$ and the constraint matrices. This was given by Özgüven [15], here written in terms of the dimensionless quantities as:

$$\tilde{\mathbf{H}}_\mathbf{C}(\tilde{\omega}) = \left[\mathbf{I} + \tilde{\mathbf{H}}_\mathbf{U}(\tilde{\boldsymbol{\omega}})\left[-\tilde{\omega}^2\tilde{\mathbf{M}}_\mathbf{C} + i\tilde{\omega}\tilde{\mathbf{C}}_\mathbf{C} + \tilde{\mathbf{K}}_\mathbf{C}\right]\right]^{-1}\tilde{\mathbf{H}}_\mathbf{U}(\tilde{\boldsymbol{\omega}}) \tag{9}$$

from which the converse relation may be inferred:

$$\tilde{\mathbf{H}}_\mathbf{U}(\tilde{\omega}) = \left[\mathbf{I} - \tilde{\mathbf{H}}_\mathbf{C}(\tilde{\boldsymbol{\omega}})\left[-\tilde{\omega}^2\tilde{\mathbf{M}}_\mathbf{C} + i\tilde{\omega}\tilde{\mathbf{C}}_\mathbf{C} + \tilde{\mathbf{K}}_\mathbf{C}\right]\right]^{-1}\tilde{\mathbf{H}}_\mathbf{C}(\tilde{\boldsymbol{\omega}}) \tag{10}$$

To obtain a convenient form for the identification of the support parameters, the left-hand side vector and the right-hand side vector are now multiplied by an external excitation $\tilde{\mathbf{f}}$. Then, taking into account that $\tilde{\mathbf{H}}_\mathbf{U}(\tilde{\omega}) = \tilde{\mathbf{y}}_\mathbf{U}(\tilde{\omega})/\tilde{\mathbf{f}}(\tilde{\omega})$:

$$\left[\tilde{\mathbf{H}}_\mathbf{C}(\tilde{\omega})^{-1} - \left[-\tilde{\omega}^2\tilde{\mathbf{M}}_\mathbf{C} + i\tilde{\omega}\tilde{\mathbf{C}}_\mathbf{C} + \tilde{\mathbf{K}}_\mathbf{C}\right]\right]\tilde{\mathbf{y}}_\mathbf{U}(\tilde{\omega}) = \tilde{\mathbf{f}}(\tilde{\omega}) \tag{11}$$

Note that, in the absence of an external excitation, Eq. (11) will be verified only at the dimensionless modal frequencies $\tilde{\omega}_{U_m} = \omega_{U_m}/\omega_{U_s}$ and corresponding mode shapes $\boldsymbol{\varphi}_{U_m}$. Then, Eq. (11) is reformulated as follows:

$$\tilde{\mathbf{H}}_\mathbf{C}(\tilde{\omega}_{U_m})^{-1}\boldsymbol{\varphi}_{U_m} = \left[-\tilde{\omega}_{U_m}^2\tilde{\mathbf{M}}_\mathbf{C} + \mathrm{i}\tilde{\omega}_{U_m}\tilde{\mathbf{C}}_\mathbf{C} + \tilde{\mathbf{K}}_\mathbf{C}\right]\boldsymbol{\varphi}_{U_m} \tag{12}$$

Notice that, from now on, for the sake of simplicity, notation will be alleviated by dropping the tildes. Assuming that the constraint matrices of the supports are diagonal, Eq. (12) can then be written in a condensed form, by extracting only those lines and columns pertaining to the system locations where constraints are applied, see [15]:

$$\mathbf{H_C}(\omega_{U_m})^{-1}\boldsymbol{\varphi}_{U_m} = \left[-\omega_{U_m}^2\mathbf{m_C} + \mathrm{i}\omega_{U_m}\mathbf{c_C} + \mathbf{k_C}\right]\boldsymbol{\varphi}_{U_m} \tag{13}$$

where $\mathbf{m_C}$, $\mathbf{c_C}$ and $\mathbf{k_C}$ stand for the reduced-sized diagonal constraint matrices at the supports. Also, from now on, it is tacitly assumed that the transfer function matrix $\mathbf{H_C}(\omega_{U_m})$ and mode shapes $\boldsymbol{\varphi}_{U_m}$ have also been downsized in order to contain only terms related to the constraint locations. Then, from Eq. (13), the following important form is obtained:

$$-\omega_{U_m}^2\mathbf{m_C} + \mathrm{i}\omega_{U_m}\mathbf{c_C} + \mathbf{k_C} = \left[\mathbf{H_C}(\omega_{U_m})\boldsymbol{\phi}_{U_m}\right]^{-1}\boldsymbol{\varphi}_{U_m} \tag{14}$$

where $\boldsymbol{\phi}_{U_m} = \mathrm{diag}(\boldsymbol{\varphi}_{U_m})$ is the diagonal matrix built from the mode shape vector $\boldsymbol{\varphi}_{U_m}$ while $\mathbf{m_C}$, $\mathbf{c_C}$ and $\mathbf{k_C}$ are vectors build from the diagonal terms of the corresponding coefficient matrices. Such trick enables one to identify the constraint parameters $\mathbf{m_C}$, $\mathbf{c_C}$ and $\mathbf{k_C}$ directly from Eq. (14), while preserving a linear identification formulation [6,16].

Concerning the real part of this complex equation, one can write Eq. (14) for two unconstrained modes $m$ and $n$:

$$-\omega_{U_m}^2 \mathbf{m_C} + \mathbf{k_C} = \mathrm{Re}\left(\left[\mathbf{H_C}(\omega_{U_m})\boldsymbol{\phi}_{U_m}\right]^{-1}\boldsymbol{\varphi}_{U_m}\right) \tag{15}$$

$$-\omega_{U_n}^2 \mathbf{m_C} + \mathbf{k_C} = \mathrm{Re}\left(\left[\mathbf{H_C}(\omega_{U_n})\boldsymbol{\phi}_{U_n}\right]^{-1}\boldsymbol{\varphi}_{U_n}\right) \tag{16}$$

In compact matrix form, Eqs. (15) and (16) become:

$$\left\{\begin{array}{c}\mathbf{m_C}\\ \mathbf{k_C}\end{array}\right\} = \left[\begin{array}{cc}-\omega_{U_m}^2\mathbf{I} & \mathbf{I}\\ -\omega_{U_n}^2\mathbf{I} & \mathbf{I}\end{array}\right]^{-1}\left\{\begin{array}{c}\mathrm{Re}([\mathbf{H_C}(\omega_{U_m})\boldsymbol{\phi}_{U_m}]^{-1}\boldsymbol{\varphi}_{U_m})\\ \mathrm{Re}([\mathbf{H_C}(\omega_{U_n})\boldsymbol{\phi}_{U_n}]^{-1}\boldsymbol{\varphi}_{U_n})\end{array}\right\} \tag{17}$$

Concerning the dissipation terms at the supports, we have directly from the imaginary part of Eq. (14):

$$\mathbf{c_C} = \frac{1}{\omega_{U_m}}\mathrm{Im}\left(\left[\mathbf{H_C}(\omega_{U_m})\boldsymbol{\phi}_{U_m}\right]^{-1}\boldsymbol{\varphi}_{U_m}\right) \tag{18}$$

### 2.2. Preconditioning technique

The identification accuracy can be improved by taking a set of $N$ unconstrained modes, which leads to the following oversized system of equations:

$$\left\{\begin{array}{c}\mathbf{m_C}\\ \mathbf{k_C}\end{array}\right\} = \left[\begin{array}{cc}-\omega_{U_1}^2\mathbf{I} & \mathbf{I}\\ \vdots & \vdots\\ -\omega_{U_N}^2\mathbf{I} & \mathbf{I}\end{array}\right]^{+}\mathrm{Re}\left(\left\{\begin{array}{c}[\mathbf{H_C}(\omega_{U_1})\boldsymbol{\phi}_{U_1}]^{-1}\boldsymbol{\varphi}_{U_1}\\ \vdots\\ [\mathbf{H_C}(\omega_{U_N})\boldsymbol{\phi}_{U_N}]^{-1}\boldsymbol{\varphi}_{U_N}\end{array}\right\}\right) \tag{19}$$

and

$$\mathbf{c_C} = \left[\begin{array}{c}\omega_{U_1}\mathbf{I}\\ \vdots\\ \omega_{U_N}\mathbf{I}\end{array}\right]^{+}\mathrm{Im}\left(\left\{\begin{array}{c}[\mathbf{H_C}(\omega_{U_1})\boldsymbol{\phi}_{U_1}]^{-1}\boldsymbol{\varphi}_{U_1}\\ \vdots\\ [\mathbf{H_C}(\omega_{U_N})\boldsymbol{\phi}_{U_N}]^{-1}\boldsymbol{\varphi}_{U_N}\end{array}\right\}\right) \tag{20}$$

where $[\otimes]^{+}$ stands for the pseudo-inverse of a general rectangular matrix $[\otimes]$ in the Moore–Penrose sense, see for instance [18].

In practice, the presence of noise in the measured transfer functions or the existence of near-nodal mode shapes at some of the measurement locations can lead to an ill-posed problem. Therefore, it is necessary to consider such feature in order to overcome this problem, which typically leads to undue measurement noise amplification and seriously corrupted identification results.

The conditioning of the formulation is already improved by scaling the formulation through dimensionless quantities, as performed starting from Eq. (6). On the other hand, the complex vector in the right hand-side of Eqs. (19) and (20) can be decomposed in the following form:

$$\left\{\begin{array}{c}[\mathbf{H_C}(\omega_{U_1})\boldsymbol{\phi}_{U_1}]^{-1}\boldsymbol{\varphi}_{U_1}\\ \vdots\\ [\mathbf{H_C}(\omega_{U_N})\boldsymbol{\phi}_{U_N}]^{-1}\boldsymbol{\varphi}_{U_N}\end{array}\right\} = \left[\begin{array}{ccc}\boldsymbol{\phi}_{U_1} & \cdots & 0\\ \vdots & \ddots & \vdots\\ 0 & \cdots & \boldsymbol{\phi}_{U_N}\end{array}\right]^{-1}\left[\begin{array}{ccc}\mathbf{H_C}(\omega_{U_1}) & \cdots & 0\\ \vdots & \ddots & \vdots\\ 0 & \cdots & \mathbf{H_C}(\omega_{U_N})\end{array}\right]^{-1}\left\{\begin{array}{c}\boldsymbol{\varphi}_{U_1}\\ \vdots\\ \boldsymbol{\varphi}_{U_N}\end{array}\right\} \tag{21}$$

### 2.3. SVD regularization

This formulation allows a better regularization of the inverse problem, in order to mitigate the presence of noise as well as numerical issues caused by near-zero in the matrix of unconstrained mode shapes. Among various methods that have been developed to overcome problems of ill-conditioning, the truncated Singular Value Decomposition (SVD) is a regularization technique that appears very elegant and effective to filter both the constrained system transfer function $\mathbf{H_C}(\omega_U)$ and the mode shape $\boldsymbol{\phi}_U$ matrices. It is possible to quantify the singularity of a given matrix through the so-called condition number, which is the ratio between the highest and the lowest singular values of the SVD matrix decomposition:

$$\boldsymbol{\Gamma} = \mathbf{U}\boldsymbol{\Sigma}\mathbf{V}^{h} \tag{22}$$

where $\boldsymbol{\Gamma}$ refers to a generic matrix to be inverted, while $\boldsymbol{\Sigma} = \mathrm{diag}(\sigma_1, \cdots, \sigma_N)$ with the singular values $\sigma_1 \geq \sigma_2 \geq .. \geq \sigma_N \geq 0$ and matrices $\mathbf{U}, \mathbf{V}$ of the left and right singular vectors are orthogonal. The superscript '$^h$' stands for the conjugate-transpose. Note that, while the condition number $c = \sigma_{\max}/\sigma_{\min}$ displays values in the range $1 \leq c \leq \infty$, the inverse of the condition number $c^* = \sigma_{\min}/\sigma_{\max}$ conveniently displays values in the range $0 \leq c^* \leq 1$. Matrix $\boldsymbol{\Gamma}$ is perfectly conditioned when $c^* = 1$ and ill-conditioned as $c^*$ decreases to zero. In terms of the matrix SVD, the pseudo-inverse transformation can be computed as:

**Table 1**
Numerical data of the rotor components.

| | | | |
|---|---|---|---|
| length of the shaft | 1.668 m | external diameter of the aluminum disks | 0.1 m |
| diameter of the shaft | 0.01 m | inner diameter of the aluminum disks | 0.01 m |
| shaft Young's modulus | 210 GPa | thickness of the aluminum disks | 0.025 m |
| shaft density | 8020 kg/m$^3$ | density of the aluminum disks | 2700 kg/m$^3$ |
| external diameter of the stainless steel disks | 0.1 m | external diameter of the aluminum disks | 0.1 m |
| inner diameter of the stainless steel disks | 0.01 m | inner diameter of the aluminum disks | 0.01 m |
| thickness of the stainless steel disks | 0.025 m | thickness of the aluminum disks | 0.005 m |
| density of the stainless steel disks | 8020 kg/m$^3$ | density of the aluminum disks | 2700 kg/m$^3$ |
| length of the bronze anchors | 0.045 m | length of the aluminum anchors | 0.032 m |
| external diameter of the bronze anchors | 0.032 m | external diameter of the aluminum anchors | 0.035 m |
| inner diameter of the bronze anchors | 0.01 m | inner diameter of the aluminum anchors | 0.01 m |
| Young's modulus of the bronze anchors | 130 GPa | Young's modulus of the aluminum anchors | 130 GPa |
| density of the bronze anchors | 8400 kg/m$^3$ | density of the aluminum anchors | 5550 kg/m$^3$ |

$$\mathbf{\Gamma}^{+} = \mathbf{V}\mathbf{\Sigma}^{+}\mathbf{U}^{h} \tag{23}$$

with $\mathbf{\Sigma}^{+} = \mathrm{diag}(1/\sigma_1, \cdots, 1/\sigma_N)$. A regularized manner to solve the inverse problem is to use a truncated pseudo-inverse Eq. (23) of the matrix $\mathbf{\Gamma}$, so that:

$$\mathbf{\Sigma}^{+}_{\mathrm{reg}} = \begin{cases} 1/\sigma_i & \text{if } \sigma_i/\sigma_{\max} \geq \varepsilon \\ 0 & \text{if } \sigma_i/\sigma_{\max} < \varepsilon \end{cases} \tag{24}$$

where $\varepsilon$ is called the truncation (filtering) boundary and the regularized pseudo-inverse is given as:

$$\mathbf{\Gamma}^{+}_{\mathrm{reg}} = \mathbf{V}\mathbf{\Sigma}^{+}_{\mathrm{reg}}\mathbf{U}^{h} \tag{25}$$

In the context of the present identification problem, the results obtained by the truncated SVD regularization technique appear effective, as illustrated in the following numerical computations. The reader may refer to [19,20] for more details about the SVD regularization.

## 3. Numerical applications

### 3.1. System description

Fig. 1 shows an experimental rig at the Applied Dynamics Laboratory (ADL) of IST/CTN, which illustrates the main features of turbo electricity generators. It is essentially composed of four spans with various lengths, each one containing two large flywheels and two thin balancing discs. This rotor model was previously studied by Baklouti et al. [17]. It is composed of a stainless steel shaft supported by six roller bearings mounted through cylindrical bronze anchors, eight thin aluminum disks maintained by cylindrical aluminum anchors, five large stainless steel disks and three large aluminum disks that have identical dimensions. Numerical data of the rotor components are shown in Table 1. Fig. 1 also illustrates a sketch of the rotor system, showing in detail the distribution of the rotor components and their dimensions.

### 3.2. Simulation results

Following the theoretical approach presented in the preceding section, the modes of the unconstrained structure were first computed using the finite element method, by solving the eigenvalue problem using the assembled matrices of the structure with free boundary conditions at the support locations. The structure was meshed using 37 beam elements, a mesh density found to be adequate with respect to the geometry of the rotor system and the modes to be used in the identification procedure. The computed modal masses $m_U$ and circular frequencies $\omega_U$, as well as the mode shapes $\boldsymbol{\varphi}_U$, are shown in Fig. 2 for the first unconstrained modes.

Next, in order to simulate the measured frequency transfer function matrix connecting the dynamics of all points of the constrained rotor, $\mathbf{H_C}(\omega)$ was numerically built from Eq. (2). For more realistic simulated measurements, random noises with Gaussian distribution and given levels were added to the corresponding impulse responses in matrix $\mathbf{h_C}(t)$, which were computed by using inverse Fourier transforms of the matrix transfer functions $\mathbf{H_C}(\omega)$. Then, noisy versions of the transfer functions were recovered from the Fourier-transformed noisy impulse responses. This manner of simulating noisy measurements is deemed realistic.

Representative transfer functions are illustrated in Fig. 3 for a relative noise level of 5% (with respect to the average RMS amplitude of the impulse responses). For compactness, only the absolute values of $\mathbf{H_C}(\omega)$ are shown. The shown plots correspond to the fourth line of the transfer function matrix, for which the rotor is excited at each support and the corresponding vibratory responses are collected at the level of the fourth support. Notice that the magnitude of noise is comparatively higher when the excitation and measurement locations are more distant. As a pre-processing step, in order to reduce the noise effect, a parabolic fitting (represented by the black curves in Fig. 3) was used to clean the transfer functions in the vicinity of the unconstrained rotor modal frequencies (represented by the vertical dashed red lines).

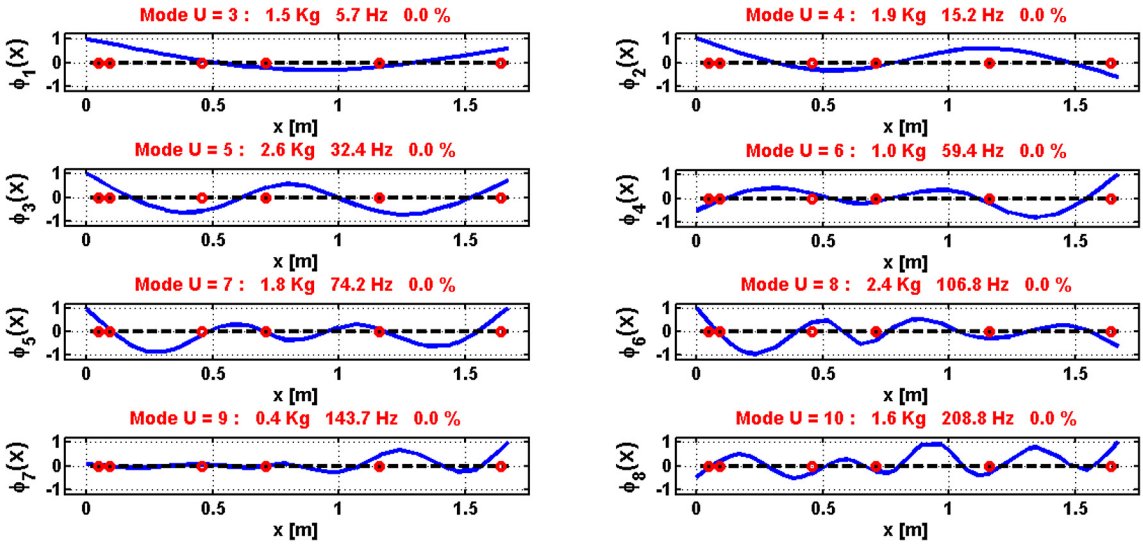


**Fig. 2.** First computed modes of the unconstrained structure.

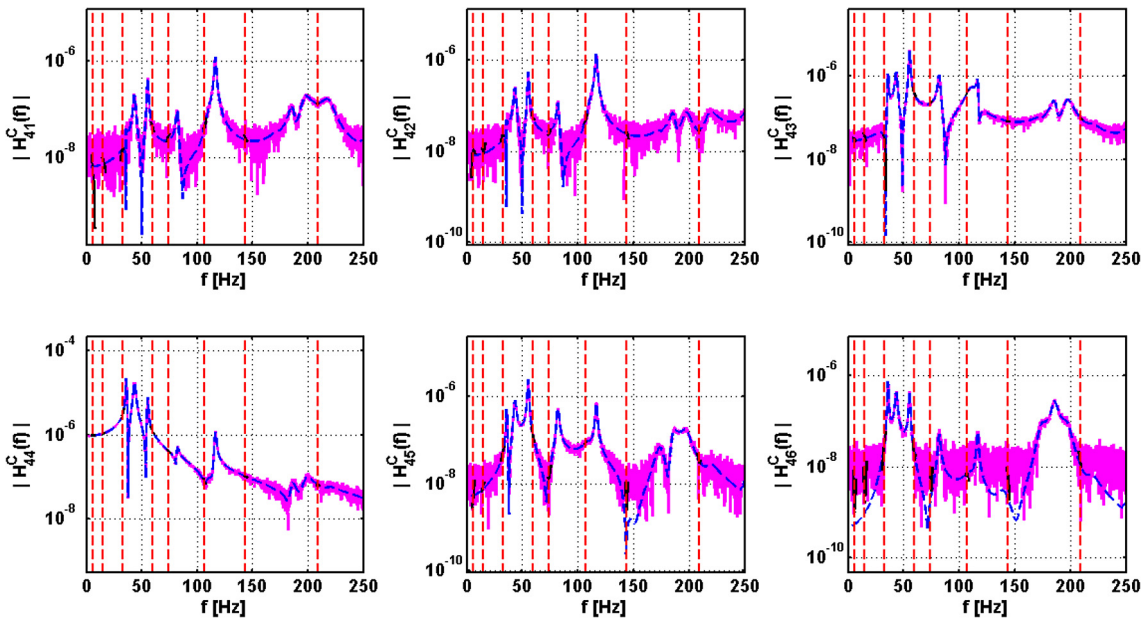


**Fig. 3.** Illustrative transfer functions measured at the fourth support. Constrained transfer functions without noise (blue); constrained transfer functions with 5% noise level (purple). The dashed lines correspond to the modal frequencies of the corresponding unconstrained system.

### 3.3. Identification results

For the identifications performed in the first example, a level of 10% noise was injected in the simulated transfer functions. The SVD regularization techniques were implemented, for filtering noise effects, as previously described. Fig. 4 presents the identification results for the various support parameters $\mathbf{m_C}$, $\mathbf{k_C}$ and $\mathbf{c_C}$, using respectively 4 and 8 modes in Eqs. (19) and (20). The green bars correspond to the simulation reference support features, while the red bars refer to the identified parameters. In this first example, all supports were assumed to be identical, with mass, stiffness and damping of the supports set to 1 kg, $10^6$ N/m and $10^3$ N s/m, respectively.

It is clear that the identification results are improved by increasing the number of unconstrained modes used. The identification errors are significantly lower, compared with the previous work by Baklouti et al. [17]. Actually, the identification strategy proposed in the present work also benefits from the dimensionless adopted formulation.

For the second example, different values of the support parameters $\mathbf{m_C}$, $\mathbf{k_C}$ and $\mathbf{c_C}$ have been assumed when building the simulated transfer functions $\mathbf{H_C}(\omega)$. Fig. 5 summarizes the identification results, for different levels of noise injected in

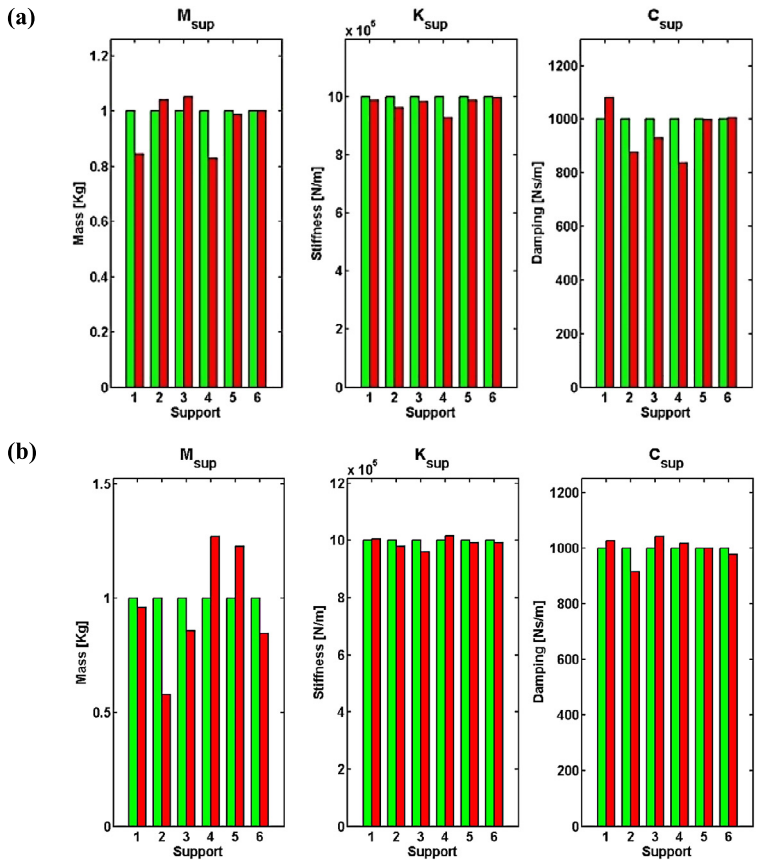


**Fig. 4.** Identification results for the various support parameters, identical for all supports, using: (a) 8 modes; (b) 4 modes, with 10% noise level.

the transfer functions (0%, 5% and 10%). One can note that the identification results are exact when no noise is added to the signals, showing that the proposed approach is consistent. The errors in the identification results become more significant when the levels of noise are increased, and this is a predictable consequence.

Overall, the proposed identification method shows satisfactory results, using the various regularization strategies previously described (SVD filtering of the identification formulation and parabolic fitting of the noisy modal peaks of the transfer functions). For the illustrative examples in this paper, by using eight unconstrained modes, the identification procedure is robust for realistic levels of noise pollution.

## 4. Conclusions

A method for the identification of supports parameters applicable to multi-span beams and rotors was developed in this work. The proposed support identification approach uses measured frequency transfer functions of the constrained system and the computed modes of the unconstrained system. An important feature of this identification formulation is that no modal identification of the constrained system is needed, as the measured transfer functions are directly used.

Inverse problems are commonly prone to numerical issues. Thus, regularization techniques have been implemented within this work to avoid ill-conditioning issues and mitigate noise effects. For the two examples provided, the proposed approach successfully led to accurate identifications of the system support parameters. Moreover, the effect of the number of modes used for the identification was discussed and a parametric study was performed in order to evaluate the robustness to noise of the identification method.

Future work involves an extension of the present identification formulation, in order to accommodate the gyroscopic and centrifugal terms arising in spinning rotor-systems.

## Acknowledgements

This work was supported by the Portuguese Foundation for Science and Technology through the bilateral agreement Portugal/Tunisia 2013–2014 (ref. 441.00).

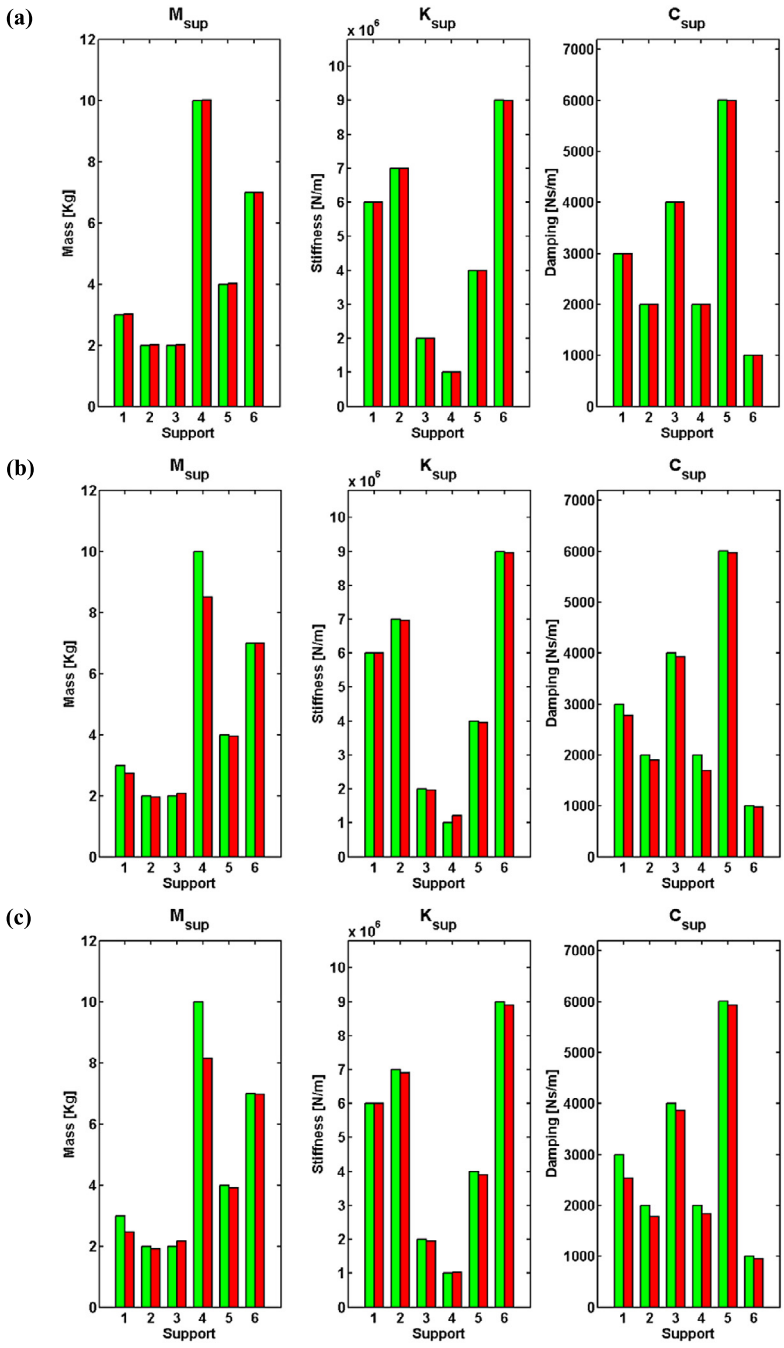


**Fig. 5.** Identification results for the various support parameters using different levels of noise: (a) 0%; (b) 5%; (c) 10%.

## References

[1] B.L. Newkirk, Shaft whipping, Gen. Elec. Rev. 27 (3) (1924) 169–178.
[2] P. Ramsden, Review of published data and their application to the design of large bearings for steam turbines, in: Proceedings of Lubrication and Wear: Fundamentals and Application to Design: A Conference, IMechE, vol. 182, 1968, pp. 75–81, Part 3A.
[3] D. Dowson, C.M. Taylor, The state of knowledge in the field of bearing-influenced rotor dynamics, Tribol. Int. 13 (5) (1980) 196–198.
[4] R. Nordmann, K. Scholhom, Identification of stiffness and damping coefficient of journal bearing by impact method, in: Proceedings of International Conference on Vibration in Rotating Machinery, vol. C285/80, Inst. Mech. Eng., 1980, pp. 231–238.
[5] S.H. Chan, M.F. White, Experimental determination of dynamic characteristics of a full size gas turbine tilting-pad journal bearing by an impact test method, in: Proc. ASME Design Engineering Division, Modal Analysis, Modeling, Diagnostics, and Control – Analytical and Experimental, vol. 38, 1991, pp. 291–298.
[6] J.H. Wang, C.M. Liou, Experimental identification of mechanical joint parameters, J. Vib. Acoust. 113 (1) (1991) 28–36.

[7] P. Arumugam, S. Swarnamani, B.S. Prabhu, Experimental identification of linearized oil film coefficients of cylindrical and tilting pad bearings, in: ASME 1994 International Gas Turbine and Aeroengine Congress and Exposition (V005T14A012-V005T14A012), American Society of Mechanical Engineers, 1994.
[8] Z.L. Qiu, A.K. Tieu, Identification of sixteen force coefficients of two journal bearings from impulse responses, Wear 212 (2) (1997) 206–212.
[9] J.H. Chen, A.C. Lee, Estimation of linearized dynamic characteristics of bearings using synchronous response, Int. J. Mech. Sci. 37 (2) (1995) 197–219.
[10] R. Tiwari, A.W. Lees, M.I. Friswell, Identification of speed-dependent bearing parameters, J. Sound Vib. 254 (5) (2002) 967–986.
[11] R. Tiwari, A.W. Lees, M.I. Friswell, Identification of dynamic bearing parameters: a review, Shock Vib. Dig. 36 (2) (2004) 99–124.
[12] O.C. De Santiago, L. San Andrés, Field methods for identification of bearing support parameters—part II: identification from rotor dynamic response due to imbalances, J. Eng. Gas Turbines Power 129 (1) (2007) 213–219.
[13] R. Tiwari, V. Chakravarthy, Simultaneous estimation of the residual unbalance and bearing dynamic parameters from the experimental data in a rotor-bearing system, Mech. Mach. Theory 44 (4) (2009) 792–812.
[14] F. Han, X. Guo, H. Gao, Bearing parameter identification of rotor-bearing system based on Kriging surrogate model and evolutionary algorithm, J. Sound Vib. 332 (11) (2013) 2659–2671.
[15] H.N. Özgüven, Structural modifications using frequency response functions, Mech. Syst. Signal Process. 4 (1990) 53–63.
[16] V. Debut, M. Carvalho, J. Antunes, Recovering the unconstrained modes of axisymmetric structures from measurements under constrained condition, in: Proc. 19th International Congress on Sound and Vibration, Vilnius, Lithuania, 2012.
[17] A. Baklouti, J. Antunes, V. Debut, T. Fakhkakh, M. Haddar, An effective method for the identification of support features in multi-supported systems, in: Advances in Acoustics and Vibration, Springer International Publishing, 2017, pp. 301–312.
[18] G.H. Golub, C.F. Van Loan, Matrix Computations, The John Hopkins University Press, Baltimore, MD, USA, 1996.
[19] V. Debut, X. Delaune, J. Antunes, Identification of the nonlinear excitation force acting on a bow string using the dynamical responses at remote locations, Int. J. Mech. Sci. 52 (2010) 1419–1436.
[20] X. Delaune, J. Antunes, V. Debut, P. Piteau, L. Borsoi, Modal techniques for the remote identification of nonlinear reaction at gap-supported tubes under turbulent excitation, J. Press. Vessel Technol. 132 (2010) 031801.